Dear Editor,

Thank you so much for your time and effort in handling our manuscript *"**Altitude-Dependent Role of Nitric Acid in Iodic Acid–Iodous Acid Nucleation: From Marine Boundary Layer Catalyst to Upper Troposphere Core Component**"* (MS No.: egusphere-2026-1771).

First, we are writing to sincerely request your permission to add a new co-author, **Xueshun Chen** (Email: chenxsh@mail.iap.ac.cn), to the revised manuscript. During the discussion stage, Xueshun Chen, affiliated with the State Key Laboratory of Atmospheric Boundary Layer Physics and Atmospheric Chemistry, Institute of Atmospheric Physics, Chinese Academy of Sciences, Beijing 100029, China, has made indispensable contributions to our research. Specifically, Xueshun Chen leveraged his expertise in aerosol microphysics and atmospheric chemistry to help us better evaluate and interpret the atmospheric implications of our theoretical data. He provided critical insights into the atmospheric relevance of our findings, helped strengthen the overall clarity, logical flow, and scientific rigor of the revised manuscript in response to the referees' constructive feedback.

Importantly, all original authors and the new author have reviewed and fully approved the addition of this co-author unanimously. We have updated the author list, affiliations, and the author contribution section in the revised manuscript accordingly. We apologize for any inconvenience this may cause and greatly appreciate your kind consideration.

Second, based on the referees' valuable comments, we have revised the manuscript carefully and listed the point-to-point responses to the reviewers' comments as follows:

Response to Referee #1

Referee's general assessment: "The authors integrate high-level quantum chemical calculations with Atmospheric Cluster Dynamics Code simulations to systematically investigate how HNO_3 influences HIO_3–HIO_2 nucleation across the troposphere. The results reveal that HNO_3 can undergo a functional transition from a nucleation catalyst in the warm marine boundary layer (MBL) to a core structural component of nucleating clusters in the cold upper troposphere (UT). This conclusion is particularly important given declining global sulfur emissions, rising marine iodine emissions, and the well-recognized significance of upper tropospheric new particle formation for the global cloud condensation nuclei budget. The manuscript is clearly written and employs state-of-the-art computational methodologies for atmospheric cluster nucleation research, while its altitude-resolved mechanistic analysis provides a valuable, novel perspective to the field. Overall, this work is logically structured and easy to follow, with a topic that aligns closely with the scope of *Atmospheric Chemistry and Physics*. I recommend this work for publication following the adequate addressing of the comments below."

Response: We sincerely thank the referee for the valuable evaluation. We have addressed every point as detailed below, with revised text highlighted in the manuscript.

Scientific issues

Comment S1. Figure 2(b) shows boundary clusters determined at 228, 248, 268, and 288 K. However, the ACDC simulations cover 204–288 K (Fig. 4a), yet boundary clusters are not provided for the remaining temperatures. Boundary clusters should be provided for all the studied temperatures.

Response: We thank the referee for this professional comment. The four temperatures (228, 248, 268, and 288 K) in Figure 2(b) were chosen as representative altitude markers (UT, FT, polar boundary layer, and MBL). Figure 2(b) documents how $c_{boundary}$ is obtained from the temperature-dependent collision and evaporation coefficients, after which the boundary clusters at any given monomer concentration can be determined. For the simulations at different altitudes in Figure 4, however, 141 distinct temperatures are required (204–288 K in 0.6 K increments), which cannot be conveniently tabulated. To ensure full reproducibility, we have therefore uploaded the full set of corresponding boundary condition files to a public repository, accessible at:

https://doi.org/10.5281/zenodo.20712556.

The repository contains the resulting $c_{boundary}$ values at every simulated temperature across 204–288 K. A corresponding sentence and citation of the repository have been added to Figure S4 of the revised SI. Additionally, we have added the representative boundary conditions to Table S3.

Comment S2. The introduction briefly notes that HNO_3 stabilizes sulfuric acid-based clusters, without explicitly extending this established behavior to iodine oxoacid systems. A clear logical bridge is missing: if HNO_3 enhances sulfuric acid nucleation via hydrogen bonding and proton transfer, it is reasonable to hypothesize a stabilizing effect in iodine oxoacid systems, given their ability to form hydrogen-bond and halogen-bond networks. Adding this analogy would strengthen the motivation for investigating HNO_3 in iodine-driven nucleation, making the hypothesis less speculative and better grounded in existing knowledge.

Response: We thank the referee for this valuable suggestion. We have linked the analogy to the existing iodine-nucleation literature, which already indicates that additional acidic/basic species participate in iodine oxoacid clustering. The added content in lines 50–54 of the revised manuscript frames HNO_3 as the natural candidate:

"Previous studies have confirmed that HNO_3 stabilizes atmospheric molecular clusters via hydrogen bonds and proton transfer-driven electrostatic interactions in both H_2SO_4–dimethylamine (DMA) (Liu et al., 2021) and H_2SO_4–NH_3 (Liu et al., 2018) nucleation systems, and since iodine oxoacids readily form hydrogen- and halogen-bond networks (Ma et al., 2023; Zu et al., 2023, 2024), the ubiquitous and co-located HNO_3 is a strong candidate for the additional species that promotes iodine-driven nucleation."

Comment S3. In Section 2.1, the cluster composition is defined as $(HNO_3)_x(HIO_3)_y(HIO_2)_z$ with $1 \le x \le 3$, but no justification is provided for limiting the number of HNO_3 molecules to three. This arbitrary cutoff lacks chemical or kinetic rationale. A brief explanation (e.g., thermodynamic or kinetic stability) should be added to clarify this constraint.

Response: We thank the referee and have added a brief explanation. Two complementary lines of evidence support the choice of $1 \le x \le 3$.

First, our calculations show that HNO_3 exhibits substantially weaker self-binding than HIO_3. As reported in Table S1, the pure-acid trimer of HNO_3 is thermodynamically unfavorable (ΔG at 268 K = + 3.9 kcal mol^{-1} for $(HNO_3)_3$), whereas the pure-acid trimer of HIO_3 is strongly favorable (ΔG at 268 K = − 23.8 kcal mol^{-1} for $(HIO_3)_3$). HNO_3 therefore cannot self-cluster effectively and must rely on participation of the base HIO_2 to form stable clusters, which limits its incorporation in nucleation.

Second, the most stable clusters in this system follow a 1:1 acid-to-base ratio, in which HNO_3 and HIO_3 act as acids and HIO_2 is the only base (Fig. 2(a)). For the studied clusters ($2 \le x + y + z \le 6$), a 1:1 acid:base composition allows at most three acid molecules, so $x \le 3$ already spans the entire thermodynamically favorable composition space. This rationale has been added to Section 2.1, lines 77–78, of the revised manuscript, as follows:

"The constraint of $1 \le x \le 3$ is applied because HNO_3 exhibits relatively weak self-binding ability (Liu et al., 2021; Zu et al., 2023), meaning HNO_3 relies on HIO_2 to form thermodynamically stable clusters."

Comment S4. In Section 2.3, the kinetic criterion $\beta c/\sum\gamma > 1$ defines stable clusters, but the monomer concentration c is not clearly specified. Given that HNO_3, HIO_3, and HIO_2 concentrations differ by orders of magnitude, an ambiguous c undermines the criterion. Please clarify whether c refers to the dominant precursor concentration or an equivalent concentration.

Response: We apologize for the ambiguity. In the criterion $\beta c/\sum\gamma > 1$, c denotes the gas-phase concentration of the specific monomer involved in the collision being evaluated; that is, each collision pathway uses the ambient concentration of the colliding species (HNO_3, HIO_3, or HIO_2) rather than a single value. We have revised Section 2.4, line 136-137 of the revised manuscript, to state this explicitly, as below:

"Here, c denotes the gas-phase concentration of the actual colliding species (HNO_3, HIO_3, or HIO_2)."

To illustrate this with a concrete example: in Figure 2(b), the reported $c_{boundary}$ is the minimum HNO_3 concentration at which an HNO_3-containing cluster reaches kinetic stability against evaporation. Once [HNO_3] exceeds the $c_{boundary}$ of, for example, the $(HNO_3)_1(HIO_3)_2(HIO_2)_3$ cluster, this cluster can successfully collide with another HNO_3 monomer to grow into $(HNO_3)_2(HIO_3)_2(HIO_2)_3$, exceeding the simulation box. The corresponding $c_{boundary}$ criteria for [HIO_3] and [HIO_2] collisions are presented in Figure S4, ensuring that each colliding species is evaluated against its own ambient concentration.

Comment S5. A previous study has shown that HIO_3–HIO_2–DMA nucleation (*Atmos. Chem. Phys.*, 24, 5823–5835, 2024) plays an important role in the marine boundary layer. This nucleation mechanism is also relevant to the Zhejiang and Mace Head cases, where DMA is abundant. To better illustrate the practical atmospheric significance of the proposed HIO_3–HIO_2–HNO_3 nucleation pathway, a direct comparison with the well-documented HIO_3–HIO_2–DMA nucleation mechanism should be included.

Response: We thank the referee for this valuable suggestion. To keep the main text focused, we have provided this direct comparison as a new figure in the revised SI (Figure S7).

At Zhejiang (288 K, high-DMA conditions, [DMA] = 1×10^8 molecules cm^{-3}) and Mace Head (288 K, [DMA] = 5×10^6 molecules cm^{-3}), we compared the cluster formation rates of the HIO_3–HIO_2–HNO_3 and HIO_3–HIO_2–DMA mechanisms across the relevant range of iodine oxoacid concentrations. The results show that at low HIO_3 concentrations (~5×10^6 molecules cm^{-3}), HIO_3–HIO_2–DMA remains the more effective pathway, whereas as HIO_3 concentrations increase, the HNO_3–HIO_3–HIO_2 mechanism takes the lead. This comparison is presented in Figure S7 of the revised SI, with the caption below:

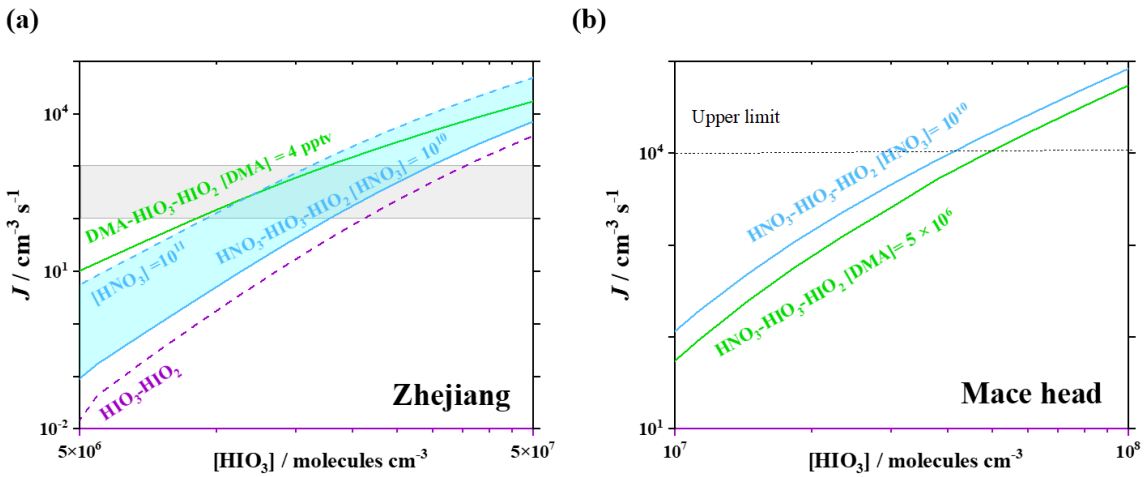

Figure S7. Cluster formation rates (J, cm^{-3} s^{-1}) for the HIO_3–HIO_2 (purple dashed line), HNO_3–HIO_3–HIO_2 (blue) and HIO_3–HIO_2–DMA (green) systems under the corresponding atmospheric conditions of (a) Zhejiang, where gray shaded areas represent locally observed cluster formation rates (Yu et al., 2019); and (b) Mace Head, where the dashed line marks the upper limit of cluster formation rates reported in field observations (Sipilä et al., 2016).

Comment S6. The conclusion links Arctic NPF enhancement to anthropogenic nitrogen emissions but does not explain how elevated HNO_3 interacts with iodine species under the cold, low-condensation-sink Arctic conditions. This weakens the causal link. Additional environmental and mechanistic context should be provided.

Response: We thank the referee for this valuable comment. We have expanded the conclusion to provide the missing mechanistic and environmental context. Specifically, we now explain how cold temperatures and a low condensation sink act together to amplify the role of HNO_3 in stabilizing iodine clusters. We have added the following explanation to lines 358–361 of the revised manuscript:

"Under cold Arctic conditions with a low condensation sink, cluster evaporation and scavenging losses are strongly suppressed, allowing HNO_3 to participate more effectively in cluster stabilization. Consequently, modest increases in HNO_3 concentrations from rising shipping NO_x emissions translate directly into substantial enhancements in the cluster formation rate."

Technical issues

We thank the reviewer for the careful reading. All listed technical corrections have been made, and similar errors found elsewhere in the manuscript have been corrected accordingly. Item-by-item responses follow.

Line 19. "200-fold enhancement in nucleation" should be "in the cluster formation rate".

Response: "200-fold enhancement in nucleation" has been corrected as "…driving a 200-fold enhancement in the cluster formation rate."

Line 48. "proton transfer-driven electrostatic interactions" should be "proton-transfer driven electrostatic

interactions".

Response: "proton transfer-driven electrostatic interactions" has been corrected as "proton-transfer driven electrostatic interactions".

Line 165. Inconsistent unit notation: "molecules/cm^3" here vs. "molecules cm^{-3}" elsewhere.

Response: "molecules/cm^3" has been corrected as "molecules cm^{-3}", and we have checked the whole manuscript and SI.

Line 196. "…minimizes scavenging of nascent clusters This enhancement…" is missing a period.

Response: "…minimizes scavenging of nascent clusters This enhancement…" has been corrected as "…minimizes scavenging of nascent clusters. This enhancement…".

Line 209. The caption refers to "Heatmaps of (a) cluster formation rates" but only one panel is labelled.

Response: Since the figure presents a single class of heatmap (a grid over *T* and CS), we have removed the "(a)".

Line 329. "solidifying HIO_3's role as a UT nucleation core component" should be "solidifying HNO_3's role…".

Response: "solidifying HIO_3's role as a UT nucleation core component" has been corrected as "…solidifying HNO_3's role as a UT nucleation core component."

Line 540. The reference Jones et al. (*Atmos. Chem. Phys.*, 2014, 14, 11843–11851) is listed but not cited in the main text.

Response: Thanks for pointing this out. We have cited Jones et al. (2014) where polar/Arctic HNO_3 is discussed.

Lines 590–595. "Li, J., Ning, A., Liu, L., and Zhang, X. … 2024a" and "… 2024b" are identical references (same title, journal, DOI).

Response: These are indeed duplicates. We have merged them into a single entry.

Response to Referee #2 (Dr. Jonas Elm)

Referee's recommendation: Zhang et al. investigates the effect of nitric acid (HNO_3) on the clustering of iodic acid (HIO_3) and iodous acid (HIO_2). The $(HIO_3)_n(HIO_2)_m$ cluster structures are taken from previous work by the same group, and the current investigation feels like a natural extension.

The cluster configurations are sampled using well-established protocols and state-of-the-art quantum chemical methods. The calculated thermochemistry is used in the atmospheric cluster dynamics code (ACDC) to simulate new particle formation (NPF) rates. Specifically, the authors simulate NPF at Zhejiang, Mace Head, Greenland and in the upper troposphere. The overall finding is that HNO_3 contributes to cluster formation in all regions. I find the altitude analysis performed in this manuscript particularly interesting and extremely well carried out. This is good inspiration for other work in the field.

I only have minor issues with the justification of the applied methods. I.e. how much can we trust that the methods are giving reliable results, without backing up the accuracy of the methods. I acknowledge that the sensitivity tests alleviate some of this concern, but it does not give the full picture.

Overall, the paper is interesting, well-written and advances our understanding of NPF in the marine environment. I believe it is a good fit for ACP and recommend publication after the following comments have been addressed.

Response: We sincerely appreciate Dr. Jonas Elm's positive feedback on our work. We highly value your constructive comments concerning the reliability and accuracy of our methods. Corresponding revisions have been made to the manuscript as suggested.

Comment 1 (Line 72). *"… with detailed procedures provided in the Supporting Information"*

I would appreciate that the sampling details are also included in the methods. Hence, integrate the "Multi-step cluster conformational search method" from the SI to the methods section as this will make it more transparent whether one can trust the found structures.

In addition, the applied UFF force field cannot handle bond breaking. Did the authors sample the cluster structures using ionic monomers to simulate bond breaking (see Kubečka et al., https://doi.org/10.1021/acs.jpca.9b03853).

Only selecting the lowest 100 cluster configurations based on PM7 could lead to the global minimum cluster being missed (see Kurfman et al., https://doi.org/10.1021/acs.jpca.1c00872). Could the authors comment on this aspect?

Response: We thank Dr. Jonas Elm for these professional comments and apologize for the previously incomplete description of the configurational sampling. We have addressed the points as follows.

(i) We have moved the multi-step conformational search method from the SI into Section 2.1 of the revised manuscript, describing the full workflow: ABCluster generation → semi-empirical PM7 pre-screening → ωB97X-D/6-311++G(3df,3pd) optimization and frequency analysis → high-level DLPNO-CCSD(T) single-point correction.

(ii) Because the UFF force field cannot describe proton transfer, we utilized ion monomers for sampling during the cluster configuration search and had manually constructed some potential stable clusters with

multiple hydrogen/halogen bonding sites based on chemical intuition. The relevant statements have been added in lines 81-84 and 87-88 of the revised manuscript as follows:

"Given the inability of the Universal Force Field (UFF) to describe proton transfer, ions in distinct protonation states were utilized to model hydrogen bonding and proton transfer. The ionic species considered include IO_3^-, NO_3^- and the protonated counterpart $H_2IO_2^+$."

"In addition, we manually constructed a set of candidate structures with multiple hydrogen- and halogen-bonding structures based on chemical intuition."

(iii) We acknowledge the limitation noted by Dr. Jonas Elm. Considering the computational cost, we retained 1000 local minima from each ABCluster search and carried forward the lowest 100 configurations based on PM7 single-point energies. As pointed out by Kurfman et al. (2021), this truncation may lead to the global minimum being missed. We have added the following statements into Section 2.1, lines 85–87, of the revised manuscript:

"Despite exhaustive sampling within the computational budget, selecting the lowest 100 configurations based on PM7 calculations may still result in the true global minimum being missed (Kurfman et al., 2021)."

Comment 2 (Line 74). *"All identified low-energy cluster conformations were rigorously optimized and subjected to frequency analysis using the Gaussian 09 package (Frisch et al., 2009) at the ωB97X-D/6-311++G(3df,3pd) (for H, O, N) + aug-cc-pVTZ-PP with ECP28MDF (for I) level of theory"*

I am missing some justification to why the ωB97X-D functional and why the 6-311++G(3df,3pd) basis set was used. There exist many benchmarks that advocate this level of theory, but without a proper reference it may seem like an arbitrary choice.

Response: We thank Dr. Jonas Elm for this constructive comment. We have added the supporting references in Section 2.2 of the revised manuscript. The ωB97X-D functional (Elm et al., 2013) together with the 6-311++G(3df,3pd) (Elm et al., 2012) basis set has been benchmarked and widely adopted for the noncovalent interactions of atmospheric molecular clusters, as it provides highly reliable estimates of binding energies.

Accordingly, we have added a sentence to explain our choice in lines 90-91 and 94-97 of the revised manuscript as follows:

"All subsequent Density Functional Theory (DFT) optimizations were performed with the Gaussian 09 package, consistently using the ωB97X-D functional and a FineGrid for integration, which has been benchmarked and widely adopted for describing noncovalent interactions in atmospheric molecular clusters (Elm et al., 2013)."

"To ensure accuracy for atmospheric systems, the 6-311++G(3df,3pd) basis set was assigned to H, O, and N, in combination with the aug-cc-pVTZ-PP basis set and ECP28MDF for I (Francl et al., 1982; Peterson et al., 2003). As demonstrated by previous benchmark studies, this combination provides highly reliable estimates of binding energies (Elm et al., 2012, 2013)."

Comment 3 (Line 80, Eq. 1). I am missing some specification on how the spin-orbit coupling SOC was calculated. Could the authors please elaborate.

In addition, I believe it was Khanniche et al. (10.1016/j.comptc.2016.09.010, https://doi.org/10.1021/acsearthspacechem.6b00010) and Engsvang et al. (https://doi.org/10.1021/acsomega.4c01235) that suggested that SOC is important for iodine species in the atmosphere. It might be worth to explicitly acknowledging the previous foundational work in the manuscript.

Response: We thank Dr. Jonas Elm for highlighting these foundational studies. As pointed out, relativistic effects are highly pronounced in systems containing heavier atoms like iodine. The foundational work establishing the importance of spin-orbit coupling (SOC) for atmospheric iodine species has been formally cited in the revised manuscript (Khanniche et al., 2016, 2017; Engsvang et al., 2024).

In this study, the spin-orbit coupling energy correction (ΔE_{SOC}) for iodine-containing clusters was obtained using Gaussian 16 as the energy difference between two single-point calculations at the 6-311++G(3df,3pd) (for H, O and N) + dhfTZVP-2c (for I): (i) a Spin-orbit DFT (SODFT) framework, which includes both the scalar potential and spin-orbit orbital potentials; and (ii) a DFT calculation using the same basis set but without spin-orbit potential. ΔE_{SOC} is calculated as the difference E(SODFT) − E(DFT). We have elaborated the SOC treatment in Section 2.2, lines 106–111, of the revised manuscript as below:

"Spin-orbit coupling (SOC) effects play a significant role in the thermodynamic properties of atmospheric iodine species due to their heavy-atom nature, as previously demonstrated by foundational studies (Khanniche et al., 2016, 2017; Engsvang et al., 2024). In this study, the SOC correction (ΔE_{SOC}) was evaluated by computing the energy difference between calculations performed with and without SOC potential. These calculations were performed using Gaussian 16 (Frisch et al., 2016) at the ωB97X-D/6-311++G(3df,3pd) (for H, N and O) + dhfTZVP-2c (for I) level of theory (Chan and Yim, 2013; Kühn and Weigend, 2015; Sarr et al., 2021; Holzer et al., 2022)"

Comment 4 (Line 83). *"… DLPNO-CCSD(T)/aug-cc-pVTZ (for H, O, and N) + aug-cc-pVTZ-PP with ECP28MDF (for I) level of theory with TightPNO and TightSCF settings."*

Engsvang et al. (https://doi.org/10.1021/acsomega.4c01235) demonstrated that relativistic effects are important to include in the Hamiltonian. Even a simple scalar relativistic method such as ZORA was found to lead to a difference. Without relativistic correction the calculated binding energies likely lead to too stable clusters. The authors should comment on this aspect.

Response: We are highly grateful to Dr. Jonas Elm for raising this crucial point regarding the relativistic effects. Based on the approach of Engsvang et al. (2024), we performed additional single-point calculations using the zeroth-order regular approximation (ZORA) employing the ORCA program. For these calculations we used the ma-ZORA-def2-TZVPP basis set for H, N, and O atoms, and the SARC-ZORA-TZVPP basis set to describe I. The ZORA-corrected cluster Gibbs free energies (ΔG_{263}) at 263 K of all optimized clusters are now reported in Table S6 below.

As shown in Table S6, ΔG_{263} obtained after ZORA correction are less negative (i.e., less stable) than the original DLPNO-CCSD(T) values, with the energy difference reaching up to ~20 kcal mol^{-1} for some of the six-molecule clusters. Using these energies, we simulated the binary HIO_3–HIO_2 cluster formation rates (J) under CLOUD chamber conditions. As shown in Figure S11, these newly obtained ZORA-corrected results (red line) were then compared with (a) the CLOUD experimental data (circles) and (b) our original DLPNO-CCSD(T) calculations (blue line). Consistent with the change in the binding energies, the J after

ZORA correction is reduced substantially, whereas the original DLPNO-CCSD(T) method demonstrates closer agreement with the CLOUD experimental results.

We have placed the ZORA-corrected ΔG_{263} and the corresponding cluster formation rates in the revised Supplementary Information (Table S6 and Figure S11, respectively) to facilitate future methodological improvements and model intercomparison. However, considering that the J simulated by the original DLPNO-CCSD(T)/aug-cc-pVTZ (for H, O, N) + aug-cc-pVTZ-PP/ECP28MDF (I) method is in better agreement with the experimental results, we have retained this approach for the single-point correction.

Correspondingly, we have included a discussion regarding the ZORA-DLPNO-CCSD(T) calculations in the Uncertainty Analysis section, lines 404–412 of the revised manuscript:

"It is also worth noting the potential uncertainties related to the relativistic effects. A recent benchmark (Engsvang et al., 2024) has demonstrated that the ZORA-DLPNO-CCSD(T) approach, which incorporates the zeroth-order regular approximation (ZORA) (Lenthe et al., 1993) provides thermodynamic estimates that are highly consistent with reference ZORA-CCSD(T) calculations. To address this, we performed single-point energy calculations at the ZORA-DLPNO-CCSD(T)/ma-ZORA-def2-TZVPP (for H, N, and O) (Neese, 2012) + SARC-ZORA-TZVPP (for I) (Rolfes et al., 2020) level of theory using the ORCA program. To provide more precise thermodynamic energies, the ZORA-corrected results are listed in Table S6, and the subsequently simulated J are presented in Figure S11. Although it includes more comprehensive physical corrections, the ZORA-corrected energies tend to yield lower J values than the CLOUD measurements. Given that DLPNO-CCSD(T) method demonstrates closer agreement, we have retained it for single-point correction."

Table S6. Gibbs free energies (ΔG) evaluated at 263 K (kcal mol^{-1}) of the $(HNO_3)_x(HIO_3)_y(HIO_2)_z$ clusters ($2 \le x + y + z \le 6$, $0 \le x \le 3$). DLPNO-CCSD(T) values were computed at the DLPNO-CCSD(T)/aug-cc-pVTZ (for H, N, O) + aug-cc-pVTZ-PP with ECP28MDF (for I) level of theory; ZORA-DLPNO-CCSD(T) values were computed at the ZORA-DLPNO-CCSD(T)/ma-ZORA-def2-TZVPP (for H, N and O) + SARC-ZORA-TZVPP (for I) level of theory, both based on geometries optimized at the ωB97X-D/6-311++G(3df,3pd) + aug-cc-pVTZ-PP level.

Clusters	ΔG_{263K} (kcal mol^{-1})	
	DLPNO-CCSD(T)	ZORA-DLPNO-CCSD(T)
$(HIO_2)_2$	-19.9	-16.0
$(HIO_2)_3$	-37.7	-30.3
$(HIO_2)_4$	-54.7	-44.4
$(HIO_2)_5$	-69.3	-54.8
$(HIO_2)_6$	-87.3	-69.3
$(HIO_3)_1(HIO_2)_1$	-18.8	-15.7
$(HIO_3)_1(HIO_2)_2$	-38.7	-32.8
$(HIO_3)_1(HIO_2)_3$	-54.6	-43.1
$(HIO_3)_1(HIO_2)_4$	-73.0	-58.5
$(HIO_3)_1(HIO_2)_5$	-76.1	-57.3
$(HIO_3)_2$	-12.8	-8.7
$(HIO_3)_2(HIO_2)_1$	-35.6	-26.8
$(HIO_3)_2(HIO_2)_2$	-54.5	-44.4
$(HIO_3)_2(HIO_2)_3$	-74.7	-60.1

$(HIO_3)_2(HIO_2)_4$	-94.0	-74.9
$(HIO_3)_3$	-25.0	-16.4
$(HIO_3)_3(HIO_2)_1$	-49.0	-39.0
$(HIO_3)_3(HIO_2)_2$	-73.7	-58.4
$(HIO_3)_3(HIO_2)_3$	-98.8	-77.7
$(HIO_3)_4$	-44.1	-31.6
$(HIO_3)_4(HIO_2)_1$	-66.9	-48.8
$(HIO_3)_4(HIO_2)_2$	-90.7	-68.9
$(HIO_3)_5$	-60.5	-42.3
$(HIO_3)_5(HIO_2)_1$	-83.5	-61.8
$(HIO_3)_6$	-74.0	-50.3
$(HNO_3)_1(HIO_2)_1$	-13.0	-10.0
$(HNO_3)_1(HIO_2)_2$	-26.3	-19.9
$(HNO_3)_1(HIO_2)_3$	-46.7	-37.2
$(HNO_3)_1(HIO_2)_4$	-62.9	-51.2
$(HNO_3)_1(HIO_2)_5$	-80.1	-64.0
$(HNO_3)_1(HIO_3)_1$	-5.3	-3.8
$(HNO_3)_1(HIO_3)_1(HIO_2)_1$	-24.6	-18.7
$(HNO_3)_1(HIO_3)_1(HIO_2)_2$	-47.3	-37.0
$(HNO_3)_1(HIO_3)_1(HIO_2)_3$	-63.8	-48.9
$(HNO_3)_1(HIO_3)_1(HIO_2)_4$	-81.6	-63.5
$(HNO_3)_1(HIO_3)_2$	-18.1	-11.2
$(HNO_3)_1(HIO_3)_2(HIO_2)_1$	-41.2	-30.7
$(HNO_3)_1(HIO_3)_2(HIO_2)_2$	-60.0	-44.8
$(HNO_3)_1(HIO_3)_2(HIO_2)_3$	-89.2	-69.2
$(HNO_3)_1(HIO_3)_3$	-32.0	-20.8
$(HNO_3)_1(HIO_3)_3(HIO_2)_1$	-55.4	-39.2
$(HNO_3)_1(HIO_3)_3(HIO_2)_2$	-81.0	-59.7
$(HNO_3)_1(HIO_3)_4$	-49.8	-31.7
$(HNO_3)_1(HIO_3)_4(HIO_2)_1$	-75.7	-55.1
$(HNO_3)_1(HIO_3)_5$	-68.1	-47.7
$(HNO_3)_2$	-0.3	1.1
$(HNO_3)_2(HIO_2)_1$	-14.8	-11.2
$(HNO_3)_2(HIO_2)_2$	-40.0	-31.4
$(HNO_3)_2(HIO_2)_3$	-55.0	-43.7
$(HNO_3)_2(HIO_2)_4$	-74.5	-58.6
$(HNO_3)_2(HIO_3)_1$	-10.3	-6.3
$(HNO_3)_2(HIO_3)_1(HIO_2)_1$	-29.7	-21.6
$(HNO_3)_2(HIO_3)_1(HIO_2)_2$	-52.4	-40.6
$(HNO_3)_2(HIO_3)_1(HIO_2)_3$	-77.7	-60.5
$(HNO_3)_2(HIO_3)_2$	-25.7	-16.4
$(HNO_3)_2(HIO_3)_2(HIO_2)_1$	-46.7	-34.0
$(HNO_3)_2(HIO_3)_2(HIO_2)_2$	-62.4	-47.9
$(HNO_3)_2(HIO_3)_3$	-37.8	-25.1
$(HNO_3)_2(HIO_3)_3(HIO_2)_1$	-61.7	-43.7
$(HNO_3)_2(HIO_3)_4$	-53.0	-36.8

$(HNO_3)_3$	2.9	4.5
$(HNO_3)_3(HIO_2)_1$	-15.1	-9.2
$(HNO_3)_3(HIO_2)_2$	-37.8	-27.3
$(HNO_3)_3(HIO_2)_3$	-59.9	-46.6
$(HNO_3)_3(HIO_3)_1$	-14.1	-7.9
$(HNO_3)_3(HIO_3)_1(HIO_2)_1$	-33.0	-24.2
$(HNO_3)_3(HIO_3)_1(HIO_2)_2$	-56.0	-41.7
$(HNO_3)_3(HIO_3)_2$	-27.0	-16.4
$(HNO_3)_3(HIO_3)_2(HIO_2)_1$	-48.7	-34.6
$(HNO_3)_3(HIO_3)_3$	-42.6	-28.3

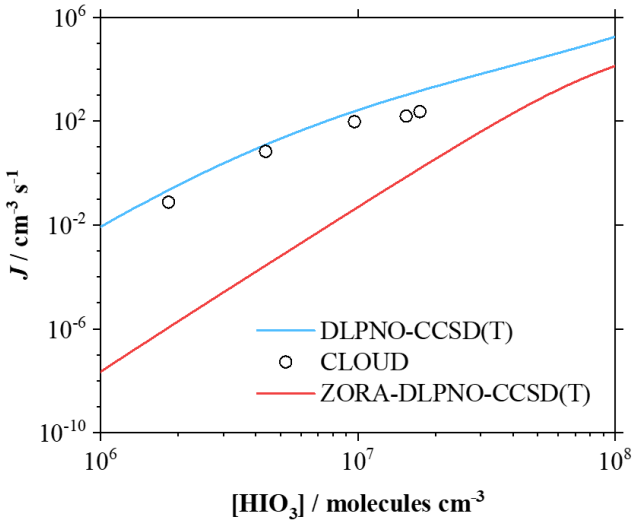

Figure S11. Cluster formation rates (J, cm^{-3} s^{-1}) of the HIO_3–HIO_2 system. Experimental data from the CLOUD chamber (He et al., 2021) are represented by circles. Theoretical ACDC simulations were evaluated at the DLPNO-CCSD(T)/aug-cc-pVTZ (for H, N, O) + aug-cc-pVTZ-PP with ECP28MDF (for I) level (blue line), and the ZORA-DLPNO-CCSD(T)/ma-ZORA-def2-TZVPP (for H, N, O) + SARC-ZORA-TZVPP (for I) level (red line). Simulations were performed under the same conditions as the CLOUD experiment: $[HIO_3] = 10^6$–10^8, $[HIO_2] = 2 \times 10^4$–2×10^6 molecules cm^{-3}, $T = 263$ K, and CS = 2.2×10^{-3} s^{-1}.

Comment 5 (Lines 108–111). Please mention the explicit boundary conditions in the main text. Setting the boundary clusters as clusters consisting of only six molecules could lead to artefacts in the ACDC simulations, giving too high cluster formation rates (see Besel et al., https://doi.org/10.1021/acs.jpca.0c03984). Too small boundary cluster will yield too high cluster formation rates. This aspect should be elaborated in the manuscript.

Response: We thank Dr. Jonas Elm for the professional comment. The previously unclear description of the boundary conditions has been rectified. The specific boundary conditions are listed in Table S3 of the revised SI. To clarify, the simulation system encompasses clusters containing up to six molecules. The

boundary conditions are seven-molecule clusters formed through the collision of a kinetically stable six-molecule cluster with one additional monomer (HNO_3, HIO_3, or HIO_2). The identity of these boundary conditions was determined individually at each simulation temperature using the $\beta c/\sum\gamma > 1$ criterion.

We have added the corresponding explanation in Section 2.4, lines 133–135, of the revised manuscript as below:

"Correspondingly, the boundary conditions are set as seven-molecule clusters, representing the smallest kinetically stable clusters that grow beyond the six-molecule simulation system."

We further acknowledge the referee's concern that, as demonstrated by Besel et al. (2020), small boundary clusters may overestimate the absolute cluster formation rate J. This effect may contribute to the modest exceedance of the field-observed upper limit discussed in our response to Comment 12.

Comment 6 (Section 3.1 and Figure 1). I do not see what Figure 1 is contributing with to the present study. It is simple chemistry to identify the donor/acceptor groups in molecules. No need for electrostatic potential maps for doing this. Please remove this part.

Instead it would be much more informative to include some of the cluster structures which are hidden in the SI.

Response: We thank Dr. Jonas Elm for this valuable suggestion. Following the referee's advice, we have moved the ESP analysis to Figure S1, and replaced it in the main text with a new Figure 1 showing representative optimized cluster structures. The new figure highlights the hydrogen bonds and halogen bonds that stabilize the $(HNO_3)_x(HIO_3)_y(HIO_2)_z$ clusters, providing a more direct chemical picture of cluster stabilization.

Comment 7 (Line 152). *"Six-molecule clusters with an acid-to-base ratio of 1:1 (HNO_3 and HIO_3 as acids, HIO_2 as base) exhibit the lowest Gibbs free energies of formation (ΔG). This 1:1 stoichiometry preference is consistent across all cluster sizes (Figure S2)."*

The 1:1 acid-to-base ratio is general finding in cluster formation studies. This was originally found by Olenius et al. (https://doi.org/10.1063/1.4819024) and generalized by Elm et al. (https://doi.org/10.1021/acs.jpca.7b08962). This finding should be put into context with previous work, as it is not a unique finding discovered here.

Response: We fully agree and apologize for not properly acknowledging the prior literature. Our work is an extension of this established finding to the HNO_3-iodine-oxoacid system. We have revised the relevant sentence, lines 180–182, to put this finding into context with previous work:

"Consistent with established thermodynamic patterns in acid-base clustering (Olenius et al., 2013; Elm, 2017), six-molecule clusters with an acid-to-base ratio of 1:1 (HNO_3 and HIO_3 as acids, HIO_2 as base) exhibit the lowest Gibbs free energies of formation (ΔG)."

Comment 8 (Line 165). *"Although HNO_3-containing clusters require a higher cboundary than HIO_3–HIO_2 clusters, ambient HNO_3 concentrations (10^8–10^{11} molecules/cm^3), spanning clean polar regions to*

polluted coastal environments"

Could you add a reference here for HNO_3 reaching 10^8 molecules cm^{-3} in clean polar regions?

Response: Thanks for the valuable suggestions. The HNO_3 concentrations of ~10^8 molecules cm^{-3} in clean polar air correspond to the measurements at Summit, Greenland (Honrath et al., 2002), as well as the Antarctic HNO_3 observations (Jones et al., 2014). To make the data sources clearer, we have explicitly added these two references corresponding to polar regions in Section 3.3, lines 216–219, of the revised manuscript:

"HNO_3 concentrations were set to 10^8–10^{11} molecules cm^{-3} (from remote polar regions (Honrath et al., 2002; Jones et al., 2014) to polluted coastal areas (Xu et al., 2018)) …"

Comment 9 (Line 174). I do not understand Figure 2(b). How can clusters that do not include HNO_3 depend on its concentration for $c_{boundary}$?

Response: We thank Dr. Jonas Elm for pointing out this inconsistency, and apologize for the confusion. We fully agree that the $c_{boundary}$ of pure HIO_3–HIO_2 clusters is independent of the HNO_3 concentration, as they do not contain HNO_3. Consequently, to prevent misleading interpretations, we have removed the pure iodine oxoacid clusters from the revised Figure 2(b). We have also refined Figure S4 by excluding the irrelevant $c_{boundary}$ thresholds for absent species, such as HIO_3 collisions involving non-HIO_3-containing clusters.

Comment 10 (Line 206). *"Given the ppb-level HNO_3 concentrations observed in the UT, this enhanced sensitivity underscores the amplified importance of HNO_3 in iodine oxoacid nucleation at high altitudes."*

Do you have a reference for HNO_3 reaching 1 ppb in the UT?

Response: Yes. The sub-ppb to ppb levels of HNO_3 concentration in the UT and tropopause regions are supported by the aircraft measurements of Jurkat et al. Specifically, their study explicitly reported that HNO_3 concentrations can exceed 1 ppb in the UT. We have cited for the precursor profiles in Section 3.4, lines 247-248:
"matching the concentration distributions of the nucleation precursors at different altitudes in the atmosphere (Jurkat et al., 2014)."

Comment 11 (Line 223). *"HIO_3 concentration was set to 1×10^7 molecules cm^{-3} in the MBL (coastal emission hotspot) (Sipilä et al., 2016) and reduced by one order of magnitude in the FT. Due to limited field constraints on HIO3 at high altitudes, its concentration was held constant above the FT."*

I am a bit concerned that the iodine oxoacid concentrations might be a bit too high in the UT. Has it actually been proven that iodine oxoacids can be transported to the upper troposphere or just been inferred? From the cited work (Twohy et al., 2002; Randel et al., 2010; Williamson et al., 2019), I only find mention of convective clouds, but not that they can transport iodine. Would iodine species formed in the lower troposphere not quite rapidly form particles and thereby be scavenged before being transported to the upper troposphere?

Response: This is an important and thoughtful concern. We acknowledge that the originally cited convective-transport references (Twohy et al., 2002; Randel et al., 2010; Williamson et al., 2019) were intended to illustrate the general physical connection between the lower and upper troposphere, and indeed did not directly address iodine concentrations at altitude. Nevertheless, iodine has been directly observed at high altitude: quantitative particulate iodine has been detected in the upper troposphere (Koenig et al., 2020), and HIO_3 along with molecular clusters have been directly measured in the marine free troposphere (Salignat et al., 2024). Given the scarcity of direct measurements of iodine oxoacids at high altitudes, the UT iodine oxoacid concentrations used in our simulations are inferred, primarily because in-situ chemical production at altitude is likely to play a significant role. Since HIO_3 can form in-situ from the IO radical (Finkenzeller et al., 2023), which exhibits a relatively altitude-invariant profile (Koenig et al., 2020), high-altitude HIO_3 can be sustained by local oxidation of IO without requiring intact uplift of HIO_3 itself. The statement in lines 254-259 of the revised manuscript is as follows:

"Due to limited field constraints on HIO_3 at high altitudes, its concentration was held constant above the FT. This assumption is based on the fact that the concentration of iodine monoxide (IO) radical, a key precursor of HIO_3 in the troposphere with relatively stable concentrations across altitudes (Koenig et al., 2020), exhibits an observed positive correlation with that of HIO_3 in the troposphere (Finkenzeller et al., 2023). HIO_2 concentration was fixed at a ratio of 1/50 relative to HIO_3 across all altitudes, consistent with the conditions in Figure 3."

Given the limited field constraints on UT iodine concentrations, we additionally performed sensitivity analyses on [HIO_3] and [HIO_2] (Figs. S7 and S8). These analyses confirm that the altitude-dependent role transition of HNO_3 from an MBL catalyst to a UT core component holds across a wide range of iodine oxoacid concentrations, including substantially lower UT values than those used in the base-case simulation. We thank the referee for this insightful comment.

Comment 12 (Line 315). *"Both HNO_3-HIO_3-HIO_2 and HIO_3-HIO_2 mechanisms are consistent with the upper limit of field-observed cluster formation rates."*

In figure 6(a) and 6(b) it is seen that both mechanisms actually exceed the observed upper limit. I suspect this could be related to too strongly binding clusters. As mentioned under methods above this could originate either from the boundary conditions or the applied quantum chemical methods. This aspect should be further commented on.

Response: We agree with Dr. Jonas Elm and have revised the wording. Instead of "consistent with the upper limit", the revised sentence now states that both mechanisms reach or modestly exceed the observed upper limit of the field-reported cluster formation rates. This modest exceedance most likely reflects two factors:

(i) Boundary-cluster size. As noted in our response to Comment 5, considering that nitric acid clusters may exhibit relatively high evaporation rates at higher temperatures, a seven-molecule boundary might not reach the critical cluster size, potentially leading to an overestimation of the absolute *J* (Besel et al., 2020).

(ii) Possible overbinding of the quantum chemical method, as suggested by a previous benchmark (Engsvang et al., 2024).

Accordingly, we have incorporated the discussion of these two potential factors into the analysis in Section 3.5, lines 346–350, of the revised manuscript:

"Both the HNO_3–HIO_3–HIO_2 and HIO_3–HIO_2 mechanisms generally reach, and at higher concentrations modestly exceed, the upper limit of field-observed cluster formation rates. This potential overestimation of *J* likely originates from methodological limitations: specifically, the finite seven-molecule boundary may not encompass the critical cluster size (Besel et al., 2020), and the applied quantum chemical level of theory might inherently produce slightly overbound clusters (Engsvang et al., 2024)."

Comment 13 (Line 344). I commend the authors for making a section on the potential uncertainties in the quantum chemical results and applied concentration. However, based on previous benchmarks, it should be explicitly stated that it is more likely that the applied methods are yielding too low free energies. Hence, the +1 kcal/mol scenario is probably the most likely.

Response: We thank Dr. Jonas Elm for this valuable suggestion. We have added a statement in Section 3.6, lines 391–393, of the revised manuscript:

"As indicated by prior benchmarks (Schmitz and Elm, 2020; Engsvang et al., 2024), the DLPNO-CCSD(T) method may slightly underestimate ΔG (i.e., over-bind the clusters). Therefore, the +1 kcal mol^{-1} perturbation is likely the most realistic scenario."

We have tried our best to address all of the referees' comments, and we believe the manuscript has been substantially improved. All major changes are highlighted in the revised manuscript. We thank the referees again for the valuable and constructive feedback.

Sincerely,

Xiuhui Zhang
Key Laboratory of Cluster Science, Ministry of Education of China
School of Chemistry and Chemical Engineering, Beijing Institute of Technology
Beijing 100081, P. R. China
Email: zhangxiuhui@bit.edu.cn

References

Besel, V., Kubečka, J., Kurtén, T., and Vehkamäki, H.: Impact of Quantum Chemistry Parameter Choices and Cluster Distribution Model Settings on Modeled Atmospheric Particle Formation Rates, J. Phys. Chem. A, 124, 5931–5943, https://doi.org/10.1021/acs.jpca.0c03984, 2020.

Chan, B. and Yim, W.-L.: Accurate Computation of Cohesive Energies for Small to Medium-Sized Gold Clusters, J. Chem. Theory Comput., 9, 1964–1970, https://doi.org/10.1021/ct400047y, 2013.

Elm, J.: Elucidating the Limiting Steps in Sulfuric Acid–Base New Particle Formation, J. Phys. Chem. A, 121, 8288–8295, https://doi.org/10.1021/acs.jpca.7b08962, 2017.

Elm, J., Bilde, M., and Mikkelsen, K. V.: Assessment of Density Functional Theory in Predicting Structures and Free Energies of Reaction of Atmospheric Prenucleation Clusters, J. Chem. Theory Comput., 8, 2071–2077, https://doi.org/10.1021/ct300192p, 2012.

Elm, J., Bilde, M., and Mikkelsen, K. V.: Assessment of binding energies of atmospherically relevant clusters, Phys. Chem. Chem. Phys., 15, 16442, https://doi.org/10.1039/c3cp52616j, 2013.

Engsvang, M., Wu, H., and Elm, J.: Iodine Clusters in the Atmosphere I: Computational Benchmark and Dimer Formation of Oxyacids and Oxides, ACS Omega, 9, 31521–31532, https://doi.org/10.1021/acsomega.4c01235, 2024.

Finkenzeller, H., Iyer, S., He, X.-C., Simon, M., Koenig, T. K., Lee, C. F., Valiev, R., Hofbauer, V., Amorim, A., Baalbaki, R., Baccarini, A., Beck, L., Bell, D. M., Caudillo, L., Chen, D., Chiu, R., Chu, B., Dada, L., Duplissy, J., Heinritzi, M., Kemppainen, D., Kim, C., Krechmer, J., Kürten, A., Kvashnin, A., Lamkaddam, H., Lee, C. P., Lehtipalo, K., Li, Z., Makhmutov, V., Manninen, H. E., Marie, G., Marten, R., Mauldin, R. L., Mentler, B., Müller, T., Petäjä, T., Philippov, M., Ranjithkumar, A., Rörup, B., Shen, J., Stolzenburg, D., Tauber, C., Tham, Y. J., Tomé, A., Vazquez-Pufleau, M., Wagner, A. C., Wang, D. S., Wang, M., Wang, Y., Weber, S. K., Nie, W., Wu, Y., Xiao, M., Ye, Q., Zauner-Wieczorek, M., Hansel, A., Baltensperger, U., Brioude, J., Curtius, J., Donahue, N. M., Haddad, I. E., Flagan, R. C., Kulmala, M., Kirkby, J., Sipilä, M., Worsnop, D. R., Kurten, T., Rissanen, M., and Volkamer, R.: The gas-phase formation mechanism of iodic acid as an atmospheric aerosol source, Nat. Chem., 15, 129–135, https://doi.org/10.1038/s41557-022-01067-z, 2023.

Frisch, M. J., Trucks, G. W., Schlegel, H. B., Scuseria, G. E., Robb, M. A., Cheeseman, J. R., Scalmani, G., Barone, V., Mennucci, B., Petersson, G. A., Nakatsuji, H., Caricato, M., Li, X., Hratchian, H. P., Izmaylov, A. F., Bloino, J., Zheng, G., Sonnenberg, J. L., Hada, M., Ehara, M., Toyota, K., Fukuda, R., Hasegawa, J., Ishida, M., Nakajima, T., Honda, Y., Kitao, O., Nakai, H., Vreven, T., Montgomery, J. A., Peralta, J. E., Ogliaro, F., Bearpark, M., Heyd, J. J., Brothers, E., Kudin, K. N., Staroverov, V. N., Kobayashi, R., Normand, J., Raghavachari, K., Rendell, A., Burant, J. C., Iyengar, S. S., Tomasi, J., Cossi, M., Rega, N., Millam, J. M., Klene, M., Knox, J. E., Cross, J. B., Bakken, V., Adamo, C., Jaramillo, J., Gomperts, R., Stratmann, R. E., Yazyev, O., Austin, A. J., Cammi, R., Pomelli, C., Ochterski, J. W., Martin, R. L., Morokuma, K., Zakrzewski, V. G., Voth, G. A., Salvador, P., Dannenberg, J. J., Dapprich, S., Daniels, A. D., Farkas, O., Foresman, J. B., Ortiz, J. V., Cioslowski, J., and Fox, D. J.: Gaussian 16, Revision A.03; Gaussian, Inc.: Wallingford CT, https://gaussian.com/citation_a03/ (last access:19 March 2026), 2016.

Holzer, C., Franzke, Y. J., and Pausch, A.: Current density functional framework for spin–orbit coupling, J. Chem. Phys., 157, 204102, https://doi.org/10.1063/5.0122394, 2022.

Honrath, R. E., Lu, Y., Peterson, M. C., Dibb, J. E., Arsenault, M. A., Cullen, N. J., and Steffen, K.: Vertical fluxes of NO_x, HONO, and HNO_3 above the snowpack at Summit, Greenland, Atmos. Environ., 36, 2629–

2640, https://doi.org/10.1016/S1352-2310(02)00132-2, 2002.

Jones, A. E., Brough, N., Anderson, P. S., and Wolff, E. W.: HO_2NO_2 and HNO_3 in the coastal Antarctic winter night: a "lab-in-the-field" experiment, Atmos. Chem. Phys., 14, 11843–11851, https://doi.org/10.5194/acp-14-11843-2014, 2014.

Jurkat, T., Voigt, C., Kaufmann, S., Zahn, A., Sprenger, M., Hoor, P., Bozem, H., Müller, S., Dörnbrack, A., Schlager, H., Bönisch, H., and Engel, A.: A quantitative analysis of stratospheric HCl, HNO_3, and O_3 in the tropopause region near the subtropical jet, Geophys. Res. Lett., 41, 3315–3321, https://doi.org/10.1002/2013GL059159, 2014.

Khanniche, S., Louis, F., Cantrel, L., and Černušák, I.: A theoretical study of the microhydration of iodic acid ($HOIO_2$), Comput. Theor. Chem., 1094, 98–107, https://doi.org/10.1016/j.comptc.2016.09.010, 2016.

Khanniche, S., Louis, F., Cantrel, L., and Černušák, I.: Thermochemistry of HIO_2 Species and Reactivity of Iodous Acid with OH Radical: A Computational Study, ACS Earth Space Chem., 1, 39–49, https://doi.org/10.1021/acsearthspacechem.6b00010, 2017.

Koenig, T. K., Baidar, S., Campuzano-Jost, P., Cuevas, C. A., Dix, B., Fernandez, R. P., Guo, H., Hall, S. R., Kinnison, D., Nault, B. A., Ullmann, K., Jimenez, J. L., Saiz-Lopez, A., and Volkamer, R.: Quantitative detection of iodine in the stratosphere, Proc. Natl. Acad. Sci. U.S.A., 117, 1860–1866, https://doi.org/10.1073/pnas.1916828117, 2020.

Kühn, M. and Weigend, F.: Two-component hybrid time-dependent density functional theory within the Tamm-Dancoff approximation, J. Chem. Phys., 142, 034116, https://doi.org/10.1063/1.4905829, 2015.

Kurfman, L. A., Odbadrakh, T. T., and Shields, G. C.: Calculating Reliable Gibbs Free Energies for Formation of Gas-Phase Clusters that Are Critical for Atmospheric Chemistry: $(H_2SO_4)_3$, J. Phys. Chem. A, 125, 3169–3176, https://doi.org/10.1021/acs.jpca.1c00872, 2021.

Lenthe, E. V., Baerends, E. J., and Snijders, J. G.: Relativistic regular two-component Hamiltonians, The Journal of Chemical Physics, 99, 4597–4610, https://doi.org/10.1063/1.466059, 1993.

Liu, L., Li, H., Zhang, H., Zhong, J., Bai, Y., Ge, M., Li, Z., Chen, Y., and Zhang, X.: The role of nitric acid in atmospheric new particle formation†, Phys. Chem. Chem. Phys., https://doi.org/10.1039/c8cp02719f, 2018.

Liu, L., Yu, F., Du, L., Yang, Z., Francisco, J. S., and Zhang, X.: Rapid sulfuric acid–dimethylamine nucleation enhanced by nitric acid in polluted regions, Proc. Natl. Acad. Sci. U.S.A., 118, e2108384118, https://doi.org/10.1073/pnas.2108384118, 2021.

Ma, F., Xie, H.-B., Zhang, R., Su, L., Jiang, Q., Tang, W., Chen, J., Engsvang, M., Elm, J., and He, X.-C.: Enhancement of Atmospheric Nucleation Precursors on Iodic Acid-Induced Nucleation: Predictive Model and Mechanism, Environ. Sci. Technol., 57, 6944–6954, https://doi.org/10.1021/acs.est.3c01034, 2023.

Neese, F.: The ORCA program system, WIREs Comput. Mol. Sci., 2, 73–78, https://doi.org/10.1002/wcms.81, 2012.

Olenius, T., Kupiainen-Määttä, O., Ortega, I. K., Kurtén, T., and Vehkamäki, H.: Free energy barrier in the growth of sulfuric acid–ammonia and sulfuric acid–dimethylamine clusters, J. Chem. Phys., 139, 084312, https://doi.org/10.1063/1.4819024, 2013.

Rolfes, J. D., Neese, F., and Pantazis, D. A.: All-electron scalar relativistic basis sets for the elements Rb–Xe, J. Comput. Chem., 41, 1842–1849, https://doi.org/10.1002/jcc.26355, 2020.

Salignat, R., Rissanen, M., Iyer, S., Baray, J.-L., Tulet, P., Metzger, J.-M., Brioude, J., Sellegri, K., and Rose, C.: Measurement report: Insights into the chemical composition and origin of molecular clusters and potential precursor molecules present in the free troposphere over the southern Indian Ocean: observations from the Maïdo Observatory (2150 m a.s.l., Réunion), Atmos. Chem. Phys., 24, 3785–3812, https://doi.org/10.5194/acp-24-3785-2024, 2024.

Sarr, S., Graton, J., Rahali, S., Montavon, G., and Galland, N.: Delocalized relativistic effects, from the viewpoint of halogen bonding, Phys. Chem. Chem. Phys., 23, 4064–4074, https://doi.org/10.1039/D0CP05840H, 2021.

Schmitz, G. and Elm, J.: Assessment of the DLPNO Binding Energies of Strongly Noncovalent Bonded Atmospheric Molecular Clusters, ACS Omega, 5, 7601–7612, https://doi.org/10.1021/acsomega.0c00436, 2020.

Sipilä, M., Sarnela, N., Jokinen, T., Henschel, H., Junninen, H., Kontkanen, J., Richters, S., Kangasluoma, J., Franchin, A., Peräkylä, O., Rissanen, M. P., Ehn, M., Vehkamäki, H., Kurten, T., Berndt, T., Petäjä, T., Worsnop, D., Ceburnis, D., Kerminen, V.-M., Kulmala, M., and O'Dowd, C.: Molecular-scale evidence of aerosol particle formation via sequential addition of HIO_3, Nature, 537, 532–534, https://doi.org/10.1038/nature19314, 2016.

Xu, W., Liu, L., Cheng, M., Zhao, Y., Zhang, L., Pan, Y., Zhang, X., Gu, B., Li, Y., Zhang, X., Shen, J., Lu, L., Luo, X., Zhao, Y., Feng, Z., Collett Jr., J. L., Zhang, F., and Liu, X.: Spatial–temporal patterns of inorganic nitrogen air concentrations and deposition in eastern China, Atmos. Chem. Phys., 18, 10931–10954, https://doi.org/10.5194/acp-18-10931-2018, 2018.

Yu, H., Ren, L., Huang, X., Xie, M., He, J., and Xiao, H.: Iodine speciation and size distribution in ambient aerosols at a coastal new particle formation hotspot in China, Atmos. Chem. Phys., 19, 4025–4039, https://doi.org/10.5194/acp-19-4025-2019, 2019.

Zu, H., Zhang, S., Liu, L., and Zhang, X.: The vital role of sulfuric acid in iodine oxoacids nucleation: impacts of urban pollutants on marine atmosphere, Environ. Res. Lett., https://doi.org/10.1088/1748-9326/ad193f, 2023.

Zu, H., Chu, B., Lu, Y., Liu, L., and Zhang, X.: Rapid iodine oxoacid nucleation enhanced by dimethylamine in broad marine regions, Atmos. Chem. Phys., 24, 5823–5835, https://doi.org/10.5194/acp-24-5823-2024, 2024.